

## Statistical improvement in detection level of gravitational microlensing events from their light curves

Ichsan Ibrahim<sup>1,4,6</sup>, Hakim L. Malasan<sup>1,3</sup>, Chatief Kunjaya<sup>1,5</sup>, Anton Timur Jaelani<sup>1,7</sup>, Gerhana Puannandra Putri<sup>1</sup> and Mitra Djamal<sup>2</sup>

<sup>1</sup> Department of Astronomy, Institute of Technology Bandung, Bandung, Indonesia; [ichsan.ibrahim@sitb.ac.id](mailto:ichsan.ibrahim@sitb.ac.id)

<sup>2</sup> Department of Physics, Department of Astronomy, Institute of Technology Bandung, Bandung, Indonesia

<sup>3</sup> Bosscha Astronomical Observatory, Department of Astronomy, Institute of Technology Bandung, Lembang, Indonesia

<sup>4</sup> Department of Informatics, STMIK-Indonesia Mandiri, Bandung, Indonesia

<sup>5</sup> Universitas Ma Chung, Malang, Indonesia

<sup>6</sup> Faculty of Shariah, Institut Agama Islam Ternate, Ternate, North Molucca, Indonesia

<sup>7</sup> Astronomical Institute, Tohoku University, Sendai, Japan

Received 2016 May 19; accepted 2017 December 13

**Abstract** In astronomy, the brightness of a source is typically expressed in terms of magnitude. Conventionally, the magnitude is defined by the logarithm of received flux. This relationship is known as the Pogson formula. For received flux with a small signal to noise ratio (S/N), however, the formula gives a large magnitude error. We investigate whether the use of Inverse Hyperbolic Sine function (hereafter referred to as the Asinh magnitude) in the modified formulae could allow for an alternative calculation of magnitudes for small S/N flux, and whether the new approach is better for representing the brightness of that region. We study the possibility of increasing the detection level of gravitational microlensing using 40 selected microlensing light curves from the 2013 and 2014 seasons and by using the Asinh magnitude. Photometric data of the selected events are obtained from the Optical Gravitational Lensing Experiment (OGLE). We found that utilization of the Asinh magnitude makes the events brighter compared to using the logarithmic magnitude, with an average of about  $3.42 \times 10^{-2}$  magnitude and an average in the difference of error between the logarithmic and the Asinh magnitude of about  $2.21 \times 10^{-2}$  magnitude. The microlensing events OB140847 and OB140885 are found to have the largest difference values among the selected events. Using a Gaussian fit to find the peak for OB140847 and OB140885, we conclude statistically that the Asinh magnitude gives better mean squared values of the regression and narrower residual histograms than the Pogson magnitude. Based on these results, we also attempt to propose a limit in magnitude value for which use of the Asinh magnitude is optimal with small S/N data.

**Key words:** gravitational lensing: micro — methods: data analysis

### 1 INTRODUCTION

Gravitational lensing is predicted by Einstein's theory of general relativity. The gravitational field of a massive object causes the light rays passing it to bend. The more massive the object, the stronger its gravitational field and

hence the greater the bending of light rays. These images may be shifted from their original locations and distorted. The effects of light deflection due to a gravitational field is called gravitational lensing. Gravitational lensing is divided into three groups (Schneider et al. 1992): (1). Strong lensing, where there are visible distortions such as

the formation of Einstein rings, arcs and multiple images. (2). Weak lensing, where the distortions of background sources are much smaller and can only be detected by analyzing large numbers of sources in a statistical way to find coherent distortions of only a few percent. The lensing shows up statistically as a preferred stretching of the background objects perpendicular to the direction of the center of the lens. (3). Microlensing, where no distortion in shape can be seen but the amount of light received from a background object changes in time as it passes behind a lens. In one typical case, stars in the Galaxy may act as the lensing objects and a star in the Galactic bulge or a remote galaxy as the background source.

For star microlensing (hereafter termed microlensing), the lensing object is a stellar mass compact object (Mao 2008). The lens is situated in the line of sight from the Earth to a background source (the top-left panel in Fig. 1). A background source radiates light rays passing the lens at different distances and directed towards the lens. The light rays will be bent at a particular bending angle that is affected by their distances to the lens. The bending angle increases with decreasing distance from the lens, and there is a unique distance such that the ray will be deflected just enough to hit the Earth. The unique distance is called the Einstein radius. If the lens moves closer to the line of sight, the effect of gravitation on light rays will be strengthened, so that the source (background) appears brighter. If the lens moves away, the background star brightness will revert to normal. Because of rotational symmetry about the Earth-source axis and when the lens, source and observer are perfectly aligned, an observer on the Earth could see the images form a ring (called an Einstein ring). An Einstein ring is centered on the ‘true’ position of the source (the projected position of the source on the plane of the sky). For any other source position, an observer on the Earth could see an image, and the source will be mapped into two annuli, one inside the Einstein ring and one outside it. In microlensing, the separation angle of the image is too small to be visible (smaller than milliarcseconds). We can observe only the change of brightness of the source as a function of time, known as the microlensing light curve (hereafter referred to as the light curve).

The light curve will have a symmetric shape if the motion of the lens, the observer and the source can be considered as linear movements. The right panel in Figure 1 shows two light curves with two impact parameters,  $(u_0) = 0.1$  and  $0.3$ . The impact parameter is

associated with the gravitational effect of the lens on light from the source which passes close to the lens. To describe the standard light curve and its parameters, the source trajectory is also shown (bottom-left panel in Fig. 1). We put the lens at the origin and the source moves along the  $x$ -axis across the line of sight. The position of the light source along the trajectory is expressed in dimensionless coordinates  $(x_s, y_s)$ . The first coordinate  $(x_s) = (t - t_0)/t_E$  and the second  $(y_s) = u_0$ . The distance between the lens and the source is  $r_s$ . From that, the impact parameter  $u_0$  (in unit time scales  $t_E$ ) is considered as the closest distance to the lens when the source moves along the trajectory. The peak time ( $t_0$ ) is the time when the light source would be closest to the lens and the time scale ( $t_E$ ) is defined as how long the source takes to traverse the Einstein ring.  $u_0, t_E$  and  $t_0$  are the parameters used to model the standard light curve (Eq. (1)).

$$A(t) = \frac{r_s(t)^2 + 2}{r_s(t) \times \sqrt{r_s(t)^2 + 4}}, \quad (1)$$

where  $A(t)$  is the magnification of brightness of a source as a function of time and  $r_s(t)$  is the distance between the lens and source as a function of time:  $r_s(t) = \sqrt{u_0^2 + (\frac{t-t_0}{t_E})^2}$ . We also note that the variability due to gravitational lensing is achromatic because photons from any wavelength will follow the same propagation path. Revitalization of research into gravitational microlensing was initiated by Paczynski (1986). The probability of observing microlensing, when we look towards the Galactic bulge, is on the order of one in a million (Udalski et al. 1994b), and in general, microlensing of a particular object is not repeatable. Therefore, it is necessary to conduct a regular and continuous survey of areas with a high density of stars or a large number of stars. The Optical Gravitational Lensing Experiment (OGLE) group is one of the research groups routinely providing data and they have implemented an early warning detection system for gravitational microlensing events (Udalski et al. 1994a).

In general, the results of photometric observations of astronomical objects provide the flux received by an observer on the Earth (hereafter referred to as the flux ( $f$ )). The flux is converted into magnitude ( $m$ ) using the Pogson equation (hereafter referred to as the conventional method).

$$m = m_0 - 2.5 \times \log f, \quad (2)$$

where  $m_0 \equiv 2.5 \times \log f_0$  and  $f_0$  is the flux of an object with magnitude 0.0.

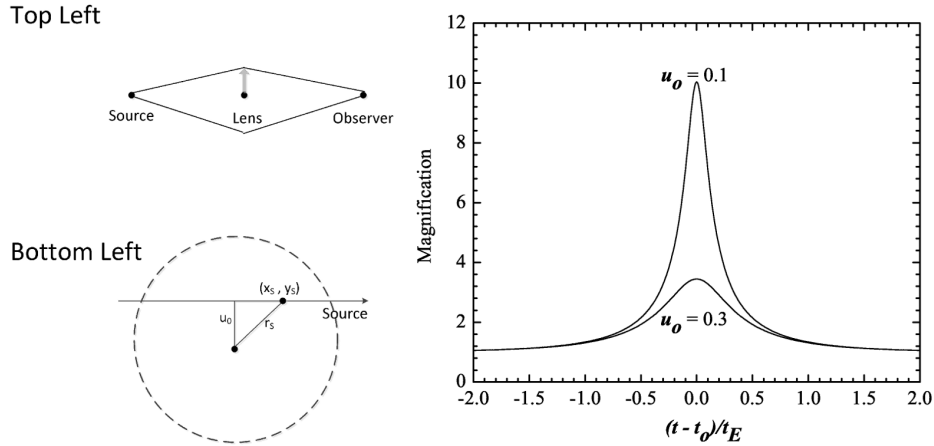


**Fig. 1** The *top-left* panel shows a side on view of the geometry of gravitational microlensing where a lens moves across the line of sight towards a background source. The *bottom-left* panel illustrates the lens position and the source trajectory. The position of an observer is in line with the plane of the lens and the source. The lens is at the origin and the source moves across the line of sight along the  $x$ -axis. The closest approach of the source ( $x_s = 0$ ) is achieved at time  $t = t_0$ , then  $r_s$  is the distance between the lens and the source and the dimensionless source position along the trajectory is given by  $x_s = (t-t_0)/t_E$  and  $y_s = u_0$  (also known as the impact parameter). The impact parameter is associated with the gravitational effect of the lens on light from the source which passes near the lens. The *right* panel shows two light curves associated with two dimensionless impact parameters of lensing events ( $u_0$ ) = 0.1 and 0.3. The time on the horizontal axis is centered on the peak time  $t_0$  when there is the closest approach of the source and is normalized to the Einstein radius crossing time  $t_E$ . (Adapted from Mao 2008).

The error of magnitude ( $\Delta m$ ) is expressed as

$$\Delta m = \left| \frac{-2.5 \times \Delta f}{f \times \ln 10} \right|. \quad (3)$$

Conversely, the error of flux ( $\Delta f$ ) can be expressed as follows

$$\Delta f = \left| \frac{f \times \Delta m \times \ln 10}{-2.5} \right|. \quad (4)$$

The Pogson formula can work well and give a reliable error of magnitude for objects with large flux. Conversely, for a small flux, which usually also means small signal to noise ratio (S/N), we will obtain a large and asymmetric error of magnitude. The error of magnitude is asymmetric because it has a non-Gaussian and skewed distribution. Therefore it is not suitable for defining the magnitude of faint objects. Lupton et al. (1999) proposed a new set of equations to define the brightness of celestial objects from the measured fluxes directly, using the Inverse Hyperbolic Sine function (Asinh) which can behave well with a small S/N as follows

$$\mu = (m_o - 2.5 \times \log b') - a \times \sinh^{-1} \left( \frac{f}{2b'} \right), \quad (5)$$

$$\text{Var}(\mu) = \frac{a^2 \times \sigma'^2}{4 \times b'^2 + f^2} \approx \frac{a^2 \times \sigma'^2}{4 \times b'^2}, \quad (6)$$

where  $\mu$  is the Asinh magnitude,  $\text{Var}(\mu)$  is the variance of the Asinh magnitude,  $a \equiv 2.5 \times \log e = 1.0857$  (Pogson ratio) with  $e = 2.7182$ .  $b' \equiv f_o \times b$  is a softening parameter used to give the same result as the Pogson formula for large flux), with  $b = \sqrt{a} \times \sigma = 1.042 \times \sigma$  being an arbitrary “softening” constant that determines the flux level at which linear behavior sets in and also as an optimal setting that balances two effects. It minimizes the differences between the Pogson and the Asinh for high S/N data and minimizes the variances for the small flux.  $\sigma' \equiv f_o \times \sigma$  is the combination of error of the flux ( $\sigma$ ) and the flux of an object at magnitude 0.0 ( $f_o$ ), and  $f$  is the flux of the object. In this work, we obtain the value of flux by using Equation (7).

This definition of magnitude has been applied in the Sloan Digital Sky Survey (SDSS) project (York et al. 2000). In 2006, the Asinh magnitude formula was used in the study of photometric standard stars at the Bosscha Observatory, Institut Teknologi Bandung (Pujijayanti et al. 2006).

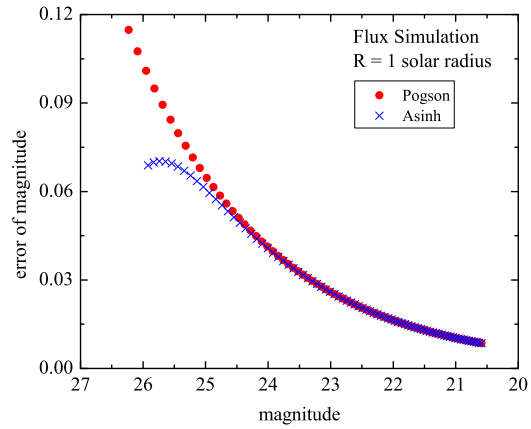


**Fig. 2** The plot of error of magnitude vs magnitude for  $1 R_{\odot}$  with stellar temperatures ranging from 3000 to 11 000 K (Ibrahim et al. 2015).

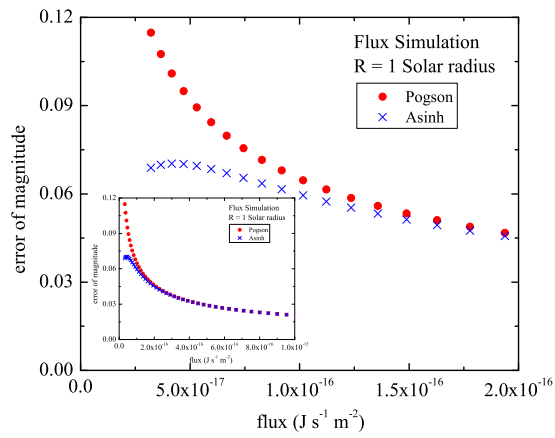


**Fig. 3** The plot of error of magnitude vs flux for  $1 R_{\odot}$  with stellar temperature ranging from 3000 to 4700 K. The flux is in  $J s^{-1} m^{-2}$ . The inset picture shows the same plot but for stellar temperatures ranging between 3000–11 000 K (Ibrahim et al. 2015).

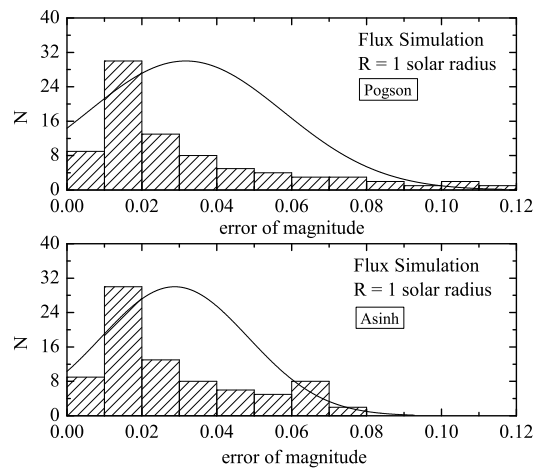


**Fig. 4** The histogram of error of magnitude for Pogson and Asinh cases (from the flux simulation for  $1 R_{\odot}$ , for stellar temperatures ranging from 3000 to 11 000 K). The line is for the normal distribution curve on binned data.

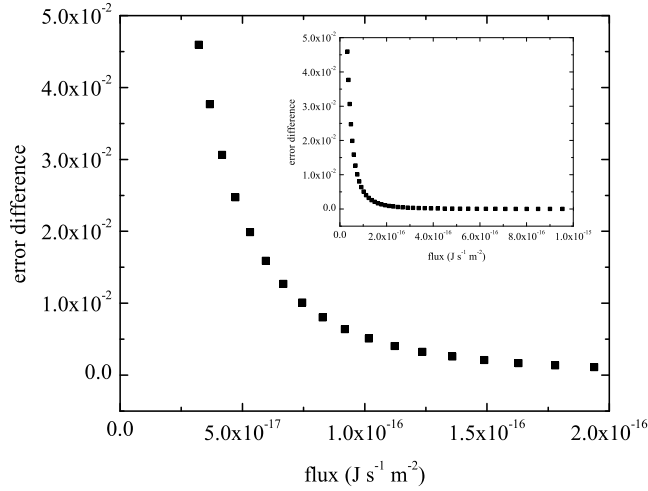


**Fig. 5** The relationship of the error difference (the Pogson error of magnitude – the Asinh error of magnitude) with flux for  $1 R_{\odot}$  and for stellar temperature range from 3000 to 4700 K. Flux is in  $\text{J s}^{-1} \text{m}^{-2}$ . The inset picture shows the same plot but for stellar temperatures ranging between 3000–11 000 K.

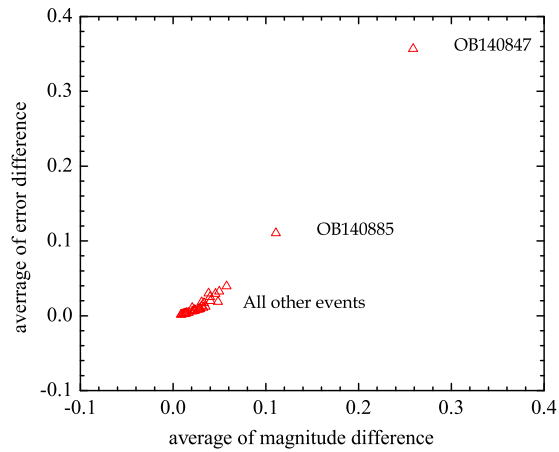


**Fig. 6** The plot of the average of the error difference and the average of the magnitude difference for 40 selected events. All the selected events (“All other events”) are grouped in an area with an average of the magnitude difference  $< 0.06$  and average of the error difference  $< 0.04$  except for two events, OB140847 and OB140885.

## 2 OBJECTIVES AND METHODOLOGY

### 2.1 Objectives

We would like to determine if the use of the Asinh magnitude gives better results and is more accurate for representing the brightness of the objects or microlensing events for small S/N photometric data, therefore increasing the possibility of detecting fainter microlensing events. In particular, for the instruments used by Early Warning System

Optical Gravitational Lensing Experiments (EWS-OGLE (<http://ogle.astrouw.edu.pl/ogle4/ews/ews.html>)), we want to find the magnitude range in which the Asinh magnitude significantly gives a better detection level than the conventional method (Pogson magnitude).

### 2.2 Methodology

In this work, we do two things: First, we simulate the flux of an object using inputs such as temperature range, size and distance of the object. Then, we chose three distinct

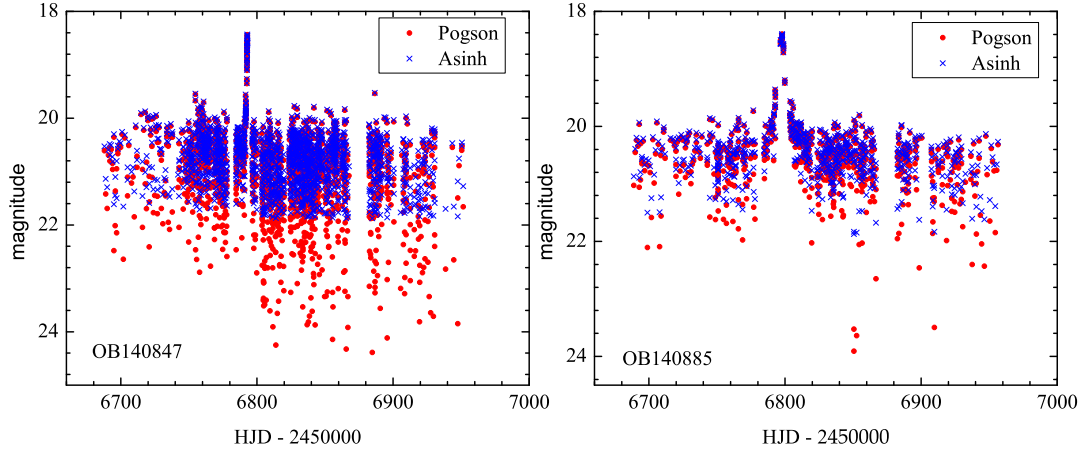


**Fig. 7** The light curve of OB140847 and OB140885 events. Both events have the largest average of magnitude difference and error difference (Table 2). The *red circles* are the Pogson magnitude and the *blue crosses* are the Asinh magnitude. The horizontal axis is (HJD–2450000) and the vertical axis is magnitude.

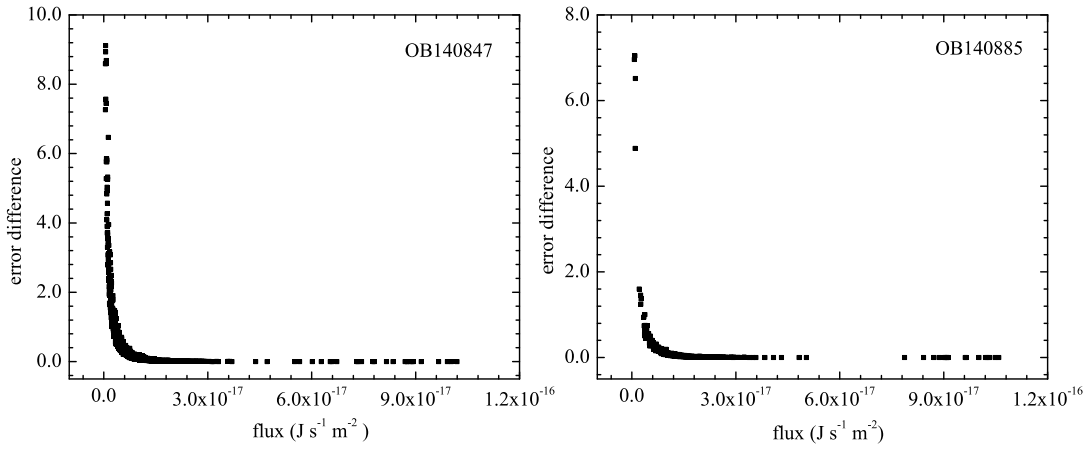


**Fig. 8** The plot of error difference (the Pogson error of magnitude – the Asinh error of magnitude) with flux for OB140847 and OB140885 events. The horizontal axis is the flux and the vertical axis is the error difference. Flux is in  $\text{J s}^{-1} \text{m}^{-2}$ .

values of stellar radii, namely 1–3 solar radii ( $R_{\odot}$ ) and stellar temperatures ranging from 3000 to 11 000 K, correlated with stars of spectral classes A to M, observed in the optical region  $\lambda = 5500 \text{ \AA}$ . In addition, we also adopt one value of light source distance,  $D = 8.5 \text{ kpc}$ . The error of the flux is derived by assuming a Poisson distribution as the distribution of the photons from the source. After calculating the flux value and the error of flux from the input data, we then calculate the Pogson magnitude ( $m$ ) and the error of magnitude ( $\Delta m$ ) using Equations (2) and (3). Subsequently, we convert the Pogson magnitude ( $m$ )

into the Asinh magnitude ( $\mu$ ) using Equation (5), and its corresponding error by taking the square root of its variance (using Eq. (6)).

Second, we also applied Equations (5) and (6) to convert photometric data of microlensing events from the EWS-OGLE database to the Pogson magnitudes ( $m$ ) and the error of magnitudes ( $\Delta m$ ), and afterwards to the Asinh magnitude ( $\mu$  and  $\Delta \mu$ ). As we could not obtain the flux from EWS-OGLE, we used Equation (7), together with information on the  $I$ -band filter from table A2 in Bessell et al. (1998, Appendix B), and the previously

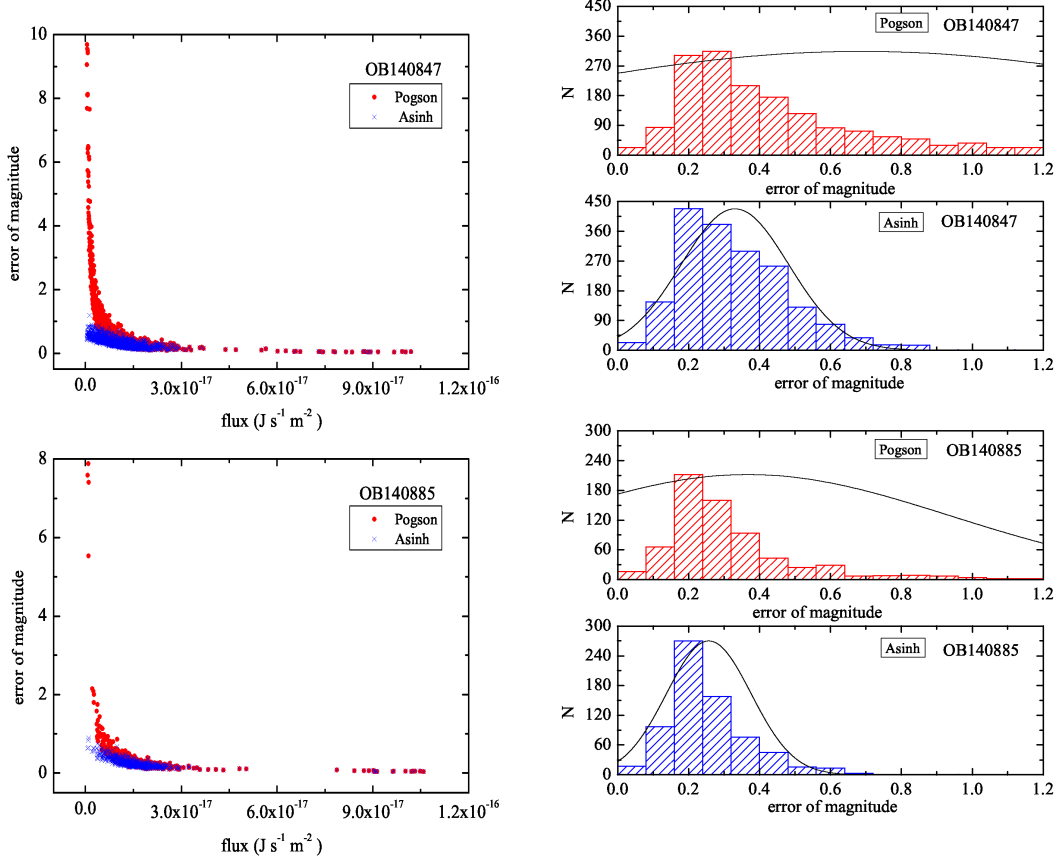


**Fig. 9** (Left panels) The plot of error of magnitude with their fluxes for OB140847 and OB140885. The range of Pogson error of magnitude is 0 to 10 for OB140847 and 0 to 8 for OB140885. The red circles are the Pogson magnitude and the blue crosses are the Asinh magnitude. (Right panel) The histograms of error of magnitude for OB140847 and OB140885. The bin sizes for all the histograms are 0.08. The ranges of Pogson error of magnitude are 0 to 10 for OB140847 and 0 to 8 for OB140885. The range of the Asinh error of magnitude for both events is 0 to 1.2. There are 125 bins for the Pogson case and 15 bins for the Asinh case. For the purposes of display in this figure, the ranges of error of magnitude are set to 0 to 1.2 for each magnitude. The line that overlays the histogram is for the normal distribution curve on binned data. The histograms of the Pogson error of magnitude are wider than those of the Asinh error of magnitude, but no closer to Gaussian than the Asinh.

calculated Pogson magnitude ( $m$ ) values to calculate the flux ( $f$ ). Next, we calculate the error of flux ( $\Delta f$ ) using Equation (4). As mentioned in Udalski et al. (2015), the  $I$ -band filter in the OGLE-IV camera that was used to collect the EWS-OGLE data very closely resembles a standard  $I$ -band filter. The equation used to calculate the flux is as follows

$$M_\lambda = -2.5 \log f_\lambda - 21.1 - z_p, \quad (7)$$

where  $M_\lambda$  is the  $I$ -band filter magnitude from EWS-OGLE,  $f_\lambda$  is the flux of the object/event and  $z_p$  is the zero point = 0.444. We compare the results between the Asinh method and conventional method, and then we give our best estimate for the magnitude range, where Asinh is

recommended to be applied as a substitute for conventional methods in which instruments are used in EWS-OGLE.

### 3 DATA

We used the photometric data of microlensing events from the EWS-OGLE database. For the purpose of this work, we selected 19 microlensing events from the 2013 season and 21 microlensing events from the 2014.  $T_{\max}$  of the first event in 2013 (OB130007) is 2456342.688 and that of the last event in 2013 (OB131785) is 2456533.251, and  $T_{\max}$  of the first selected event in 2014 (OB140042) is 245726.323 and that of the last selected event in 2014 (OB141885) is 2456914.471.  $T_{\max}$  is the

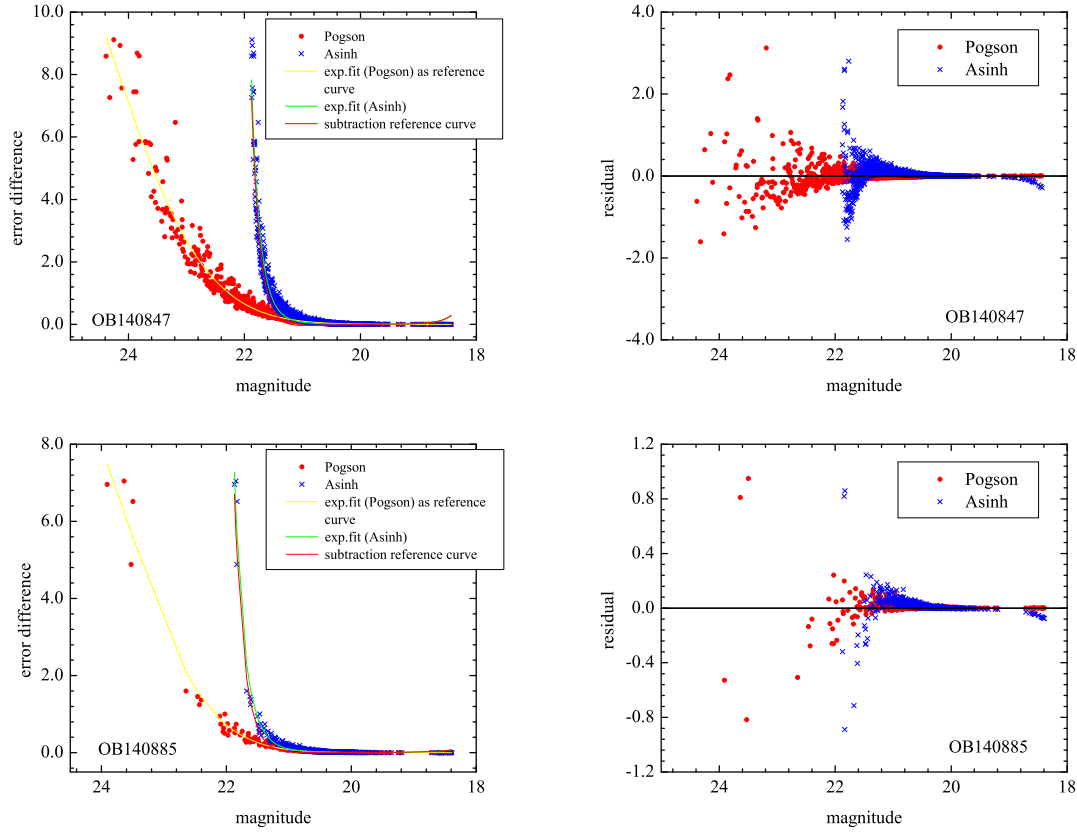


**Fig. 10** The plot of error difference (the Pogson error of magnitude – the Asinh error of magnitude) *vs* the magnitude (*left panels*) and the fitting residual plots (*right panels*) for OB140847 and OB140885 events. The *red circles* are for the Pogson case and the *blue crosses* are for the Asinh case. The *yellow line* is an exponential fit of the error difference to the Pogson magnitude and the *green line* is an exponential fit of the error difference to the Asinh magnitude. The function in Equation (8) uses the exponential fitting. Coefficients of determination for the exponential fit for the Pogson case are 0.9555 (OB140847) and 0.962 (OB140885) and for the Asinh case are 0.926 (OB140847) and 0.922 (OB140885). The exponential fits of the error difference to the Pogson magnitude are set as the reference data sets/reference curves. The exponential fit of the Asinh will be subtracted by the reference data set/curve. Before the subtraction, the two data sets would be interpolated or extrapolated. The *red line* is the result of the subtraction. From the result, what magnitudes have an error difference of about 0.001 and 0.0001 could be determined and are called “magnitude limits.”

time when the selected events reach the maximum brightness, specified in Heliocentric Julian Date (HJD). The selected events are given in Table 1. In particular, we only used *I*-band photometric data from the EWS-OGLE database. Every selected event satisfies three microlensing light curve model parameters: the maximum amplification ( $A_{\max} \leq 6.5$  (intensity units), the magnitude amplification ( $D_{\text{mag}} < 1.9$  magnitude) and the base magnitude of the source in *I*-band ( $I_0 \geq 19.5$  magnitude).

## 4 RESULTS

### 4.1 The Flux Simulation

The flux simulation with input star radius of  $1 R_{\odot}$  resulted in the lowest values of flux. The lowest fluxes

were found to produce the largest magnitude values and the largest errors in the flux. In this case, it can be seen that the Asinh formula gave a smaller error range than the Pogson equation (Figs. 2 and 3). We also found that the error of magnitude histogram for the Asinh formula is narrower than that for the conventional method (Fig. 4). Statistically, the Asinh formula gave better flux-to-magnitude transformation. Consequently, we also found that the error difference, which was defined as the difference between the Pogson error of magnitude and the Asinh error of magnitude values (the Pogson error of magnitude – the Asinh error of magnitude), increased as the flux decreased (Fig. 5).

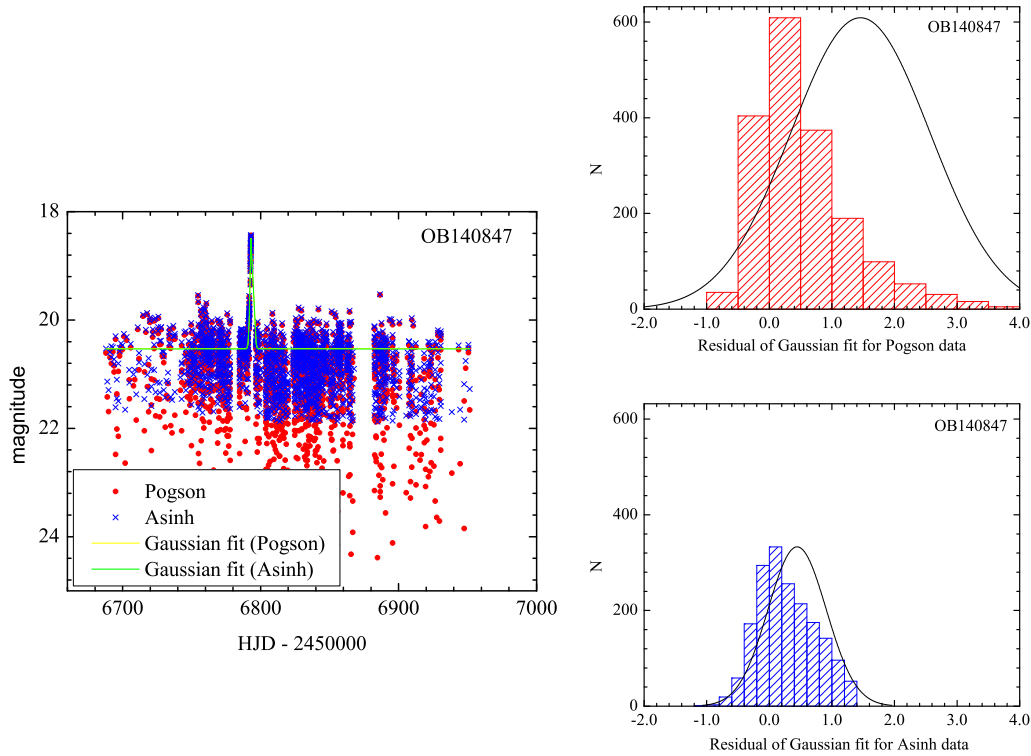


**Fig. 11** Gaussian fit for the Pogson and the Asinh data and the fitting residual histogram for OB140847. The horizontal axis is for time (HJD – 2450000) and the vertical axis is for event brightness (magnitude). The *red circles* are for the Pogson data, the *blue crosses* are for the Asinh data, the *yellow line* is for the Gaussian fitting of the Pogson data and the *green line* is for the Gaussian fitting of the Asinh data. The line that overlays the histogram is for the normal distribution curve on binned data.

#### 4.2 Photometry Data from the Selected Events

First, the photometry data of the selected events were transformed to the flux and its error. After that, we used Equations (5) and (6) to calculate the Asinh magnitude and their errors for all selected events. Because the events occur over time, there is not a single magnitude value or error value but an average over time. For analysis of selected events, we calculate the average of magnitudes and the average of the error difference. The average of the magnitude difference has a range from  $8.556 \times 10^{-3}$  to  $2.589 \times 10^{-1}$  magnitude and the average of the error difference has a range from  $1.495 \times 10^{-3}$  to  $3.567 \times 10^{-1}$  magnitude (Fig. 6).

Data on the differences are presented in Table 2. From the figure, we can see all of the selected events are grouped in an area with an average of magnitude difference  $<0.06$  and an average of error difference  $<0.04$ , except for two events, OB140847 and OB140885. Both of these events have the largest differences, the largest stan-

dard deviations of magnitude, the smallest S/N values and the faintest magnitudes among the selected events (Table 2). Because of these facts, we chose them for further analysis and light curves are presented in Figure 7. We could see that the Asinh magnitude has a smaller value than the Pogson magnitude. The range of the Asinh magnitude is about 18.4 to 21.9 for both events. However, the ranges of Pogson magnitude are about 18.4 to 24.4 (OB140847) and 18.4 to 24.0 (OB140885). Also, the Asinh magnitude gives a smaller error of magnitude than the Pogson magnitude. The largest average of the error difference is 0.357 from one event: OB140847 and the smallest is 0.002 from four events: OB130123, OB130131, OB130671 and OB131691 (Table 2). These facts can be seen more firmly in the examples given in Figure 8, which show the relationship of the error difference and the flux from both methods. The results are similar to the results from subsection 4.1. Furthermore, we compare graphs of the magnitude difference versus flux with histograms of both magnitudes. These are shown in

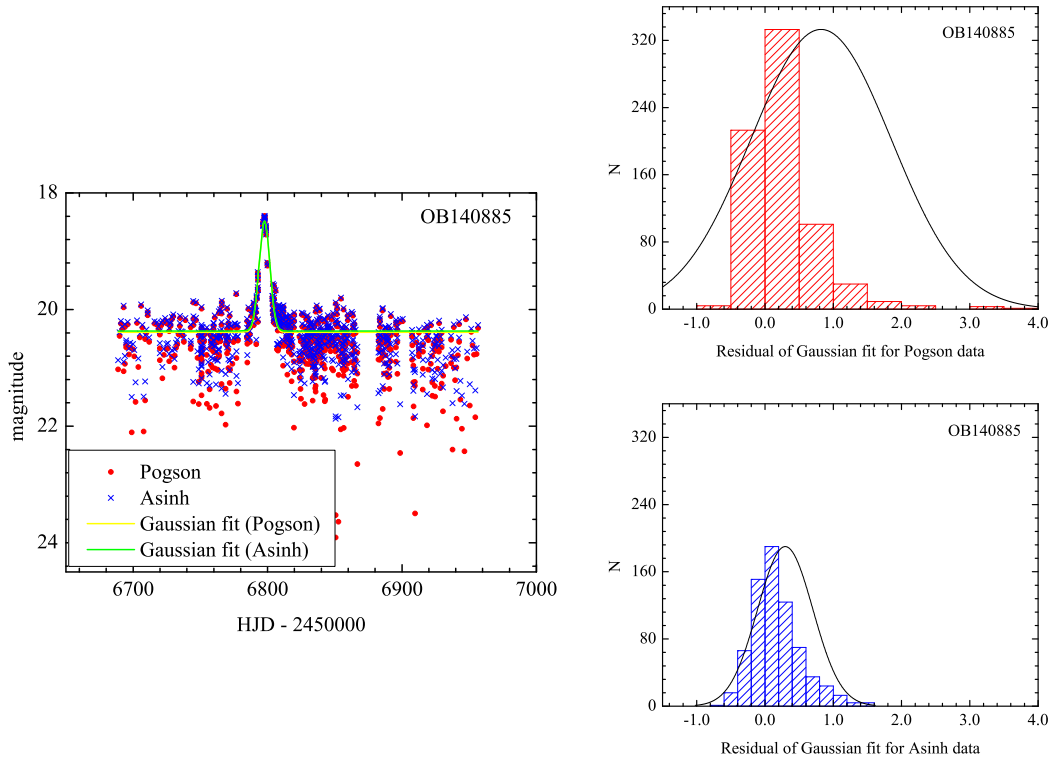


**Fig. 12** Gaussian fit for the Pogson and the Asinh data and the fitting residual histogram for OB140885. The horizontal axis is for time (HJD – 2450000) and the vertical axis is for event brightness (magnitude). The *red circles* are for the Pogson data, the *blue crosses* are for the Asinh data, the *yellow line* is for the Gaussian fitting of the Pogson data and the *green line* is for the Gaussian fitting of the Asinh data. The line that overlays the histogram is for the normal distribution curve on binned data.

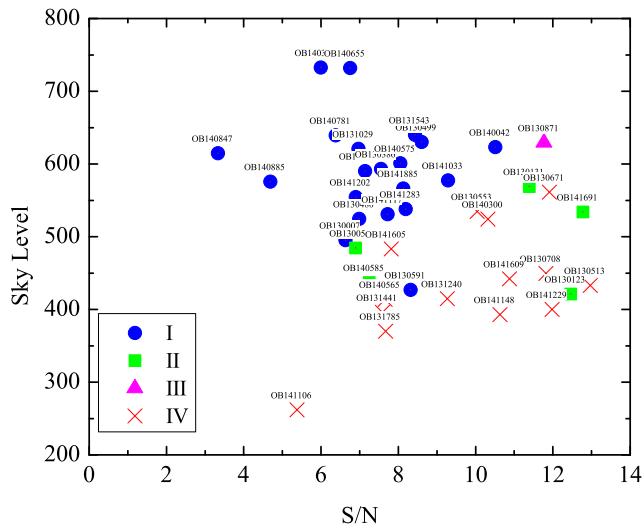


**Fig. 13** Grouping of hypothetical population test results for all the selected events. The horizontal axis is the average of the S/N and the vertical axis is the average of the sky level. *Blue circles* are for Group I, *green rectangles* are for Group II, *magenta triangles* are for Group III and *red crosses* are for Group IV. Two events that have the smallest S/N are OB140847 and OB140885. Group I has a high sky level and a small S/N. The average S/N and average sky level are presented in Table 2.

**Table 1** 40 Selected Microlensing Events from the 2013–2014 Seasons

Event	$T_{\max}$ (HJD)	$I_0$ (mag)
OB130007	2456342.688	21.255
OB130053	2456340.052	20.316
OB130123	2456334.944	19.739
OB130131	2456359.620	19.617
OB130164	2456360.641	20.130
OB130386	2456378.117	20.036
OB130480	2456393.939	21.957
OB130499	2456396.615	21.576
OB130513	2456407.534	19.846
OB130553	2456405.921	20.037
OB130591	2456407.099	20.622
OB130671	2456431.497	21.214
OB130708	2456433.665	20.419
OB130871	2456448.971	20.739
OB131029	2456457.083	20.829
OB131240	2456489.517	20.170
OB131441	2456394.300	20.387
OB131543	2456508.784	22.172
OB131785	2456533.251	20.356
OB140042	2456726.323	19.662
OB140300	2456733.427	19.985
OB140326	2456693.378	20.088
OB140565	2456761.503	20.292
OB140575	2456765.740	21.055
OB140585	2456764.259	20.262
OB140655	2456771.968	20.072
OB140781	2456785.642	21.040
OB140847	2456792.997	20.481
OB140885	2456797.602	20.410
OB141033	2456818.710	19.790
OB141106	2456820.626	20.950
OB141117	2456823.992	21.082
OB141148	2456830.665	20.052
OB141202	2456832.262	22.056
OB141229	2456833.003	20.022
OB141283	2456840.671	21.021
OB141605	2456878.619	20.299
OB141609	2456880.637	19.831
OB141691	2456887.918	20.910
OB141885	2456914.471	21.616

Notes: accessed from the OGLE site (<http://ogle.astrouw.edu.pl/ogle4/ews/ews.htm>) on 2015 June 25.

Figure 9. From the figure, we see that the histograms of the error from the Asinh case are narrower than logarithmic (Pogson).

We found another interesting result from plotting the error difference with magnitude (Fig. 10): there is a tendency that the error difference will grow rapidly for small magnitude. We want to know if there is an equation that can describe the difference error as a function of magnitude.

To find the equation, we did the curve fitting to the data set. Based on the fact that there is a tendency that the error difference will expand exponentially for small magnitude, the authors choose an exponential function (Ibrahim et al. 2015) to relate error difference ( $\delta$ ) with each magnitude ( $m$ ). The relation is given in Equation (8).

$$\delta = e^{(a+bm+cm^2)}, \quad (8)$$

**Table 2** Average Sky Levels, S/N, Statistical Data and Groupings based on a Hypothetical Population Test for 40 Selected Events

Event	Sky Level	S/N	Number of Data Points	Minimum Magnitude	Std. Dev of Magnitude	Average of Magnitude Difference	Average of Error Difference	Grouping based on Hyp. Population Test
OB130007	495.400	6.63	2675	21.198	0.258	0.033	0.011	I
OB130164	590.329	7.14	4779	21.208	0.289	0.029	0.009	I
OB130386	593.107	7.55	877	22.852	0.377	0.033	0.017	I
OB130480	524.486	6.99	5001	21.088	0.217	0.029	0.009	I
OB130499	630.454	8.60	2305	23.185	0.450	0.031	0.018	I
OB130591	426.797	8.32	1705	24.142	0.528	0.038	0.030	I
OB131029	620.714	6.97	3615	23.171	0.462	0.046	0.029	I
OB131543	640.079	8.43	5320	20.882	0.234	0.021	0.006	I
OB140042	623.243	10.51	10532	20.649	0.240	0.014	0.003	I
OB140326	732.749	5.99	2181	24.140	0.388	0.050	0.032	I
OB140575	601.018	8.05	3738	20.822	0.270	0.023	0.007	I
OB140655	732.144	6.75	2187	23.100	0.384	0.040	0.020	I
OB140781	639.498	6.38	2176	22.940	0.498	0.058	0.039	I
OB140847	614.790	3.33	1816	24.385	0.815	0.259	0.357	I
OB140885	575.835	4.69	698	23.909	0.617	0.111	0.110	I
OB141033	577.601	9.29	9376	20.659	0.263	0.017	0.004	I
OB141117	531.100	7.72	787	22.360	0.369	0.031	0.013	I
OB141202	554.643	6.90	9729	21.107	0.225	0.029	0.009	I
OB141283	538.156	8.19	5971	20.952	0.256	0.022	0.006	I
OB141885	566.310	8.13	9001	20.921	0.268	0.023	0.007	I
OB130053	484.447	6.89	778	21.162	0.327	0.035	0.012	II
OB130123	421.165	12.46	3212	20.550	0.167	0.009	0.002	II
OB130131	568.990	11.39	2902	20.570	0.223	0.011	0.002	II
OB140585	437.112	7.25	1139	21.123	0.282	0.028	0.009	II
OB141691	533.928	12.78	4193	20.402	0.151	0.009	0.002	II
OB130871	629.174	11.77	2300	22.855	0.551	0.021	0.011	III
OB130513	432.907	12.97	2367	20.964	0.486	0.013	0.003	IV
OB130553	534.685	10.04	89	22.145	0.730	0.040	0.025	IV
OB130671	561.398	11.91	996	20.274	0.211	0.010	0.002	IV
OB130708	449.479	11.82	326	20.615	0.352	0.014	0.003	IV
OB131240	414.798	9.27	865	21.586	0.410	0.023	0.008	IV
OB131441	395.931	7.59	144	20.945	0.303	0.028	0.009	IV
OB131785	369.971	7.67	172	20.964	0.329	0.027	0.008	IV
OB140300	524.202	10.32	258	20.967	0.525	0.022	0.007	IV
OB140565	413.912	7.66	467	21.092	0.337	0.028	0.009	IV
OB141106	261.888	5.38	188	21.526	0.320	0.048	0.019	IV
OB141148	392.784	10.63	268	20.506	0.331	0.015	0.003	IV
OB141229	399.928	11.98	152	20.711	0.483	0.014	0.003	IV
OB141605	483.014	7.82	510	20.938	0.272	0.024	0.007	IV
OB141609	442.155	10.88	472	20.374	0.242	0.013	0.003	IV

Notes: I. reject null hypothesis for both tests; II. reject null hypothesis for the t-test only; III. reject null hypothesis for the variance test only; IV. accept null hypothesis for both tests.

where  $\delta$  is error difference,  $m$  is magnitude,  $a$  is a constant of the function, and  $b$  and  $c$  are coefficients of the function.

Later, we found that the coefficient of determination ( $R^2$ ) of the curve fitting is always greater than 0.72 (Table 3). The smallest coefficient of determination is 0.725 (OB141691) and the largest is 0.988 (OB130553). The examples of model fitting and their residuals are pre-

sented in Figure 10. Given the goodness of fit, we could say that the error differences are dependent on their magnitude.

We fixed the data from the exponential fit of the error difference (the Pogson error of magnitude – the Asinh error of magnitude) to the Pogson magnitude as the reference data set/reference curve. We subtracted the data of the exponential fit of the error difference to the

**Table 3** Coefficients of Determination ( $R^2$ ) of Fitting for the Function  $\delta = e^{(a+bm+cm^2)}$  and Magnitude Limits for Two Values of  $|\Delta\delta| = 0.001$  and  $0.0001$  Magnitude for the Selected Events

Event	$R^2$ (the Pogson set data)	$R^2$ (the Asinh set data)	$ \Delta\delta  = 0.001$	$ \Delta\delta  = 0.0001$
OB130007	0.899	0.899	20.415	19.745
OB130053	0.948	0.948	20.431	19.850
OB130123	0.785	0.785	20.382	19.947
OB130131	0.876	0.876	20.241	19.776
OB130164	0.907	0.907	20.401	19.776
OB130386	0.943	0.944	20.282	19.968
OB130480	0.828	0.828	20.387	19.775
OB130499	0.963	0.958	20.440	18.589
OB130513	0.950	0.949	20.114	19.669
OB130553	0.988	0.988	20.335	18.318
OB130591	0.973	0.957	20.841	20.456
OB130671	0.823	0.823	20.539	19.849
OB130708	0.920	0.920	20.399	19.941
OB130871	0.942	0.942	20.448	18.668
OB131029	0.949	0.950	20.245	18.390
OB131240	0.919	0.920	20.478	19.932
OB131441	0.908	0.908	20.548	20.087
OB131543	0.854	0.854	20.309	19.823
OB131785	0.932	0.932	20.533	20.053
OB140042	0.900	0.900	20.177	19.722
OB140300	0.935	0.935	20.285	19.863
OB140326	0.949	0.922	18.951	NA
OB140565	0.935	0.935	20.504	19.997
OB140575	0.891	0.891	20.228	19.721
OB140585	0.932	0.932	20.475	19.970
OB140655	0.937	0.938	20.261	17.357
OB140781	0.946	0.948	19.894	18.524
OB140847	0.955	0.926	20.096	19.947
OB140885	0.962	0.922	20.577	20.082
OB141033	0.904	0.904	20.231	19.753
OB141106	0.949	0.949	20.780	20.327
OB141117	0.925	0.928	20.424	19.082
OB141148	0.910	0.910	20.501	20.017
OB141202	0.860	0.861	20.416	19.825
OB141229	0.949	0.949	20.505	20.037
OB141283	0.873	0.874	20.357	19.849
OB141605	0.911	0.911	20.542	20.076
OB141609	0.887	0.887	20.357	19.887
OB141691	0.725	0.725	20.137	19.794
OB141885	0.899	0.899	20.253	19.717

Asinh magnitude by the reference data set/curve. Before the subtraction, the two data sets were interpolated or extrapolated. Later, we calculated the result of the subtracted reference curve for each event (in magnitudes). Then, we could determine, from the result of subtraction, what magnitudes have an error difference of about 0.001 and 0.0001 magnitude. We called these cases ‘magnitude limits.’

To distinguish from the error difference (the Pogson error of magnitude – the Asinh error of magnitude)  $\delta$  that is used for exponential fitting from the error difference

of each magnitude (the Pogson or the Asinh magnitude), we write the result of the subtraction of the exponential fit of the error difference to the Pogson magnitude by the exponential fit of the error difference to the Asinh magnitude as  $|\Delta\delta|$ . For all the events, we were able to find the magnitude that produced  $|\Delta\delta| = 0.001$ . However, we only found magnitude limits from some events that could produce  $|\Delta\delta| = 0.0001$  (Table 3). We called these “magnitude limits.” Noting that the current limit of detectable stellar variability is on the order of  $10^{-3}$  magnitude, the error difference of all events could be significant. We

**Table 4** Parameters of Gaussian Fitting for OB140847 and OB140885

Events	mag		HJD		w		A		sigma		FWHM	
	Pogson	Asinh	Pogson	Asinh	Pogson	Asinh	Pogson	Asinh	Pogson	Asinh	Pogson	Asinh
OB140847	20.528	20.537	6793.822	6793.830	2.307	2.367	7.878	8.023	1.154	1.184	2.717	2.787
	$\pm 0.009$	$\pm 0.009$	$\pm 0.134$	$\pm 0.128$	$\pm 0.119$	$\pm 0.115$	$\pm 0.882$	$\pm 0.831$				
OB140885	20.391	20.367	6797.654	6797.666	8.040	8.085	19.216	19.086	4.020	4.042	9.467	9.519
	$\pm 0.012$	$\pm 0.011$	$\pm 0.097$	$\pm 0.104$	$\pm 0.176$	$\pm 0.184$	$\pm 0.464$	$\pm 0.475$				

strongly recommended using the Asinh magnitude for EWS-OGLE data when the magnitude is about 20.343 or fainter.

## 5 DISCUSSION AND CONCLUSIONS

Generally, from the curve fitting, the results from the conventional method look similar to those from the Asinh method. In order to find out whether the data produced from the two approaches are distinguishable, we carried out some hypothetical population testing to determine if the Pogson dataset and the Asinh dataset come from the same population. We used a two-sample t-test and a variance test. The null hypothesis assumes that the data sets are the same. For the t-test, no mean difference between the data sets would indicate that the null hypothesis is true, while a mean difference would support the alternative hypothesis. For the variance test, no variance difference would indicate that the null hypothesis is true, while a ratio of variances larger than 1 would support the alternative hypothesis.

After performing the tests, we found that 20 out of the 40 selected events reject the null hypothesis for both tests, and hence we conclude that the difference between the Pogson dataset and the Asinh dataset is significant. We then divided the selected events into four groups: Group I contains those events that reject the null hypothesis for both tests. Group II contains those events that reject the null hypothesis for the t-test only. Group III contains those events that reject the null hypothesis for the variance test only and Group IV contains those events that accept the null hypothesis for both tests. We also found that, in general, the average S/N for the 20 selected events (in Group I) is smaller than that for the other events. The results are presented in Table 2 and Figure 13. The results of the population tests indicate why half of the selected events exhibit similarity in the residual plots from the curve fitting.

By looking at the error difference (error of Pogson – error of Asinh) vs. flux plots (similar to Fig. 8), it is clear that for larger fluxes, there are no significant differ-

ences in magnitude or their error between the two methods. However, this is not the case for small fluxes. The Asinh method is found to give a smaller deviation than the Pogson method for the low flux region. The result is similar to that described by Lupton et al. (1999). We also found that the average of the magnitude difference between the two methods is on the order of 0.01 magnitude and the error of magnitude from the Asinh method is always smaller than that given by the conventional method. The average of error difference is on the order of  $10^{-2}$  magnitude. At what limit would we recommend using the Asinh rather than the conventional method? For the instrument used by the OGLE project, the limit is 20.343 magnitude. Fainter than that and the Asinh will be better than the conventional method. It is possible to conduct a similar experiment with other instrument systems, to define their magnitude limits.

We speculate as to why there are 20 events that have a large error and hence for them the Asinh is more appropriate.

Firstly, they have the faintest magnitude among our selected samples and a high sky level. For example, we can see from Table 2 that the event OB140847 has the faintest magnitude = 24.385 and sky level = 614.79. After examining photometric data from EWS-OGLE further, it could be seen, in general, that the average sky level during the observation is higher than for other groups (Table 2). This makes the S/N ratio for these objects smaller than the other groups. The two lowest S/N ratios are 3.33 (OB140847) and 4.69 (OB140885). Another factor that needs to be considered is the number of data points. This factor places OB141106 (with number of data points = 188) into Group IV as well as having small S/N. From these, we conclude there is a combination of several factors such as magnitude, sky level, S/N and number of data points from the events that result in 20 events requiring use of the Asinh magnitude.

Secondly, from the result of fitting the magnitude data with the Gaussian function to find the peak of the light curve, there is an indication that the Asinh magni-

**Table 5** Reduced  $\chi^2$  Values and Mean Squared Values of Regression for All 40 Events

Event	Reduced $\chi^2$		Mean square of regression	
	Pogson	Asinh	Pogson	Asinh
OB130007	1.932	1.969	275696.298	274779.060
OB130053	2.250	2.305	80236.593	79945.576
OB130123	2.530	2.536	311715.348	311414.225
OB130131	4.052	4.070	277186.127	276847.378
OB130164	3.366	3.438	484705.459	483196.018
OB130386	3.415	3.536	88346.643	88020.296
OB130480	1.634	1.654	510575.351	509087.324
OB130499	2.835	2.947	230040.380	229246.443
OB130513	3.903	3.928	222143.196	221833.259
OB130553	4.324	4.601	8737.589	8695.142
OB130591	3.990	4.173	174324.506	173560.100
OB130671	2.185	2.190	96111.616	96008.103
OB130708	2.947	2.968	32078.768	32029.962
OB130871	3.476	3.578	222270.709	221729.266
OB131029	2.762	2.924	366430.207	364577.547
OB131240	6.485	6.557	86489.845	86273.990
OB131441	1.817	1.835	14903.523	14862.271
OB131543	2.612	2.639	528581.444	527444.711
OB131785	2.204	2.225	17689.260	17641.428
OB140042	5.656	5.686	1005100.000	1003590.000
OB140300	11.629	11.704	24852.776	24789.817
OB140326	2.109	2.201	221161.787	219998.985
OB140565	2.691	2.731	47870.199	47731.523
OB140575	3.289	3.328	369299.063	368392.245
OB140585	2.392	2.426	116803.418	116464.628
OB140655	6.227	6.313	219163.844	218219.644
OB140781	2.097	2.265	225303.874	223904.455
OB140847	1.559	2.232	200588.902	195193.664
OB140885	1.453	1.701	73576.156	72716.726
OB141033	2.588	2.609	948392.481	946693.061
OB141106	1.011	1.028	20487.846	20391.489
OB141117	2.293	2.386	80180.387	79913.648
OB141148	2.386	2.393	26674.681	26633.978
OB141202	1.652	1.677	997291.035	994322.924
OB141229	4.304	4.328	14935.737	14913.643
OB141283	2.682	2.718	597310.478	595925.593
OB141605	1.778	1.798	52394.528	52266.290
OB141609	3.250	3.262	46030.650	45969.895
OB141691	2.208	2.214	399176.806	398818.338
OB141885	2.664	2.716	892879.282	890699.829

tude is statistically better than the Pogson magnitude for small S/N data. The parameters of Gaussian fitting for OB140847 and OB140885 data are presented in Table 4. Other results show that the Asinh magnitude fitting residual histograms are narrower than those of the Pogson magnitude (Figs. 11 and 12). In other words, by using the Asinh magnitude, we can determine a more certain base magnitude for each event compared to the Pogson magnitude.

The reduced  $\chi^2 = 2.232$  (for the Asinh data) is higher than 1.559 (for the Pogson data) from OB140847

and 1.707 (for the Asinh data) is similarly higher than 1.453 (for the Pogson data) from OB140885, but the mean squared values of the regression of the Asinh magnitude were found to be smaller than those of the Pogson magnitude. These results also support the use of Asinh magnitude for small S/N data. The reduced  $\chi^2$  values and the mean squared values of the regression for all 40 events are shown in Table 5. This study provides hope that we could detect microlensing events from a noisier observation when using the Asinh method. If we can retrieve the raw data from the EWS-OGLE database, there

is a possibility of discovering other microlensing events from fainter stars. We also hope that our work could be of significant help to observatories which suffer from an increasingly more light-polluted observation environment, such that they could obtain more valuable signals from fainter stars.

**Acknowledgements** The authors wish to thank DIKTI Kementerian Riset Teknologi dan Pendidikan Tinggi for the 2014 research grant with contract number: 1062d/I1.C0I/PL/2014. This paper is a part of Ichsan Ibrahim's dissertation in the Astronomy Graduate Program of Institute of Technology Bandung.

## References

- Bessell, M. S., Castelli, F., & Plez, B. 1998, *A&A*, 333, 231
- Ibrahim, I., Malasan, H. L., Djamal, M., et al. 2015, *Publication of Korean Astronomical Society*, 30, 235
- Lupton, R. H., Gunn, J. E., & Szalay, A. S. 1999, *AJ*, 118, 1406
- Mao, S. 2008, in *Proceedings of the Manchester Microlensing Conference*, ed. E. Kerins, S. Mao, N. Rattenbury and L. Wyrzykowski, 1
- Paczynski, B. 1986, *ApJ*, 304, 1
- Pujijayanti, R., Kunjaya, C., Malasan, H. L., Nugraha, S. D., Kristyowati, D., 2006, in *Proceeding International Conference Mathematics and Natural Science(ICMNS)-2008*, 1228, <https://www.scribd.com/document/370036073/Standard-Star-Observation-by-Incorporating-Asinh-Magnitude-at-The-Bosscha-Observatory-Pujijayanti-et-al-2006>
- Schneider, P., Ehlers, J., & Falco, E. E. 1992, *Gravitational Lenses* (Berlin: Springer-Verlag), 1
- Udalski, A., Szymanski, M., Kaluzny, J., et al. 1994a, *Acta Astronomica*, 44, 227
- Udalski, A., Szymanski, M., Stanek, K. Z., et al. 1994b, *Acta Astronomica*, 44, 165
- Udalski, A., Szymański, M. K., & Szymański, G. 2015, *Acta Astronomica*, 65, 1
- York, D. G., Adelman, J., Anderson, Jr., J. E., et al. 2000, *AJ*, 120, 1579